Using TEM and SEM to unveil the role of nanoclays in polymer blends

M. F. Almeida, A.V. Machado, and J. A. Covas

Institute for Polymers and Composites/I3N, University of Minho, Campus de Azurém 4800-058 Guimarães, Portugal

This work investigates the dispersion of montmorillonite (MMT) in a polymer matrix, in order to create a nanocomposite. *PA/PP/¿* clay (70/30/5, *w/w/ phr*) and PA/PP/PP-g-MA/clay (70/30/5/5, w/w/phr/phr), containing either Cloisite C15A or C30B commercial organoclays, were probed in terms of compatibilization effects and blend performance. The nanocomposites were melt blended in a co-rotating twin screw extruder under fixed operating conditions, samples being collected on-line for subsequent study. SEM and TEM images provided a detailed view of morphology and nanoclay dispersion, thus helping to clarify the eventual compatibilizing effect of the latter. Generally, SEM revealed a large reduction in domain size when both organoclays were used, yielding a finer dispersed phase, although distinct dispersion and compatibilization mechanisms seem to exist. Despite of the enhanced level of exfoliation reached with Cloisite C30B suspended in the PA6 phase shown by TEM, blends with Cloisite C15A seemed to exhibit a higher compatibilization level.

Keywords microscopy; organoclay; nanocomposites; blending; compatibilization.

Introduction

The preparation, characterization and application of polymer matrix based nanocomposites is currently a very dynamic area of research due to the growing number of reports showing that the incorporation of small percentages of layered clays, carbon nanotubes, carbon nanofibres, graphene, polyhedral oligomeric silsesquixanes (POSS), metal oxide particles, layered titanates, nanowhiskers, among others, may provide spectacular gains in terms of mechanical and barrier properties, flammability resistance, electrical/electronic properties and polymer blend compatibilization. In particular, exfoliated clays seem to be particularly suited for mechanical property enhancement, decreased gas permeability, flammability resistance, promotion of degradability of biodegradable polymers and compatibilization [15]. Also, as with other nano-size particles, the overall crystallization rate and the glass transition temperature are also affected. These improved properties result from the high aspect ratio of these fillers and from the interaction between them and the matrix.

The preparation of nanocomposites from clays and nanoclays can follow various routes (including in situ polymerization, solution and latex methods [6-11]), but melt compounding is the most popular, as it uses processing technologies that are relatively well understood (very often, twin screw extrusion), automatable and

with a good production yield, scalable between the laboratory and production environments and thus with economical advantages.

Generally, the aim of the operation is to obtain complete dispersion and distribution of the clay in the polymer matrix, i.e., complete exfoliation of the clay platelets and their homogeneous spatial arrangement within the matrix. However, in practice, this morphology is seldom (if ever) achieved, different degrees of dispersion being obtained (i.e., with varying degree of penetration of the polymer chains into the silicate galleries), depending on the type of equipment, operating conditions and polymer/clay type and characteristics [12-15]. Therefore, it is not only important to understand how the macroscopic properties change with the nanoscale level of the nanocomposite morphology, but also what are the dispersion mechanisms developing in processing equipment and how to control them. In any case, it is very important to be able to characterize properly the existing morphology.

Wide-angle X-ray scattering, WAXS, is one of the most popular methods to probe nanocomposites, as it is relatively simple to use. The spectrum of a composite with zero clay dispersion should be similar to that of the original clay, i.e., with a characteristic peak indicating a certain platelet separation (d-spacing). For a completely exfoliated clay no peak is expected, since there is no longer a regular spacing between platelets. At intermediate dispersion states, a peak should be present, but shifted to lower 2θ angles (larger d-spacing) than that of the original peak. However, interpretation of WAXS may be deceptive, as many factors may influence the analysis of the scans. For instance, the absence of a peak is not conclusive evidence of exfoliation [11, 16]. Small angle X-Ray scattering, solid-state NMR and neutron scattering have also been used, but only on a limited basis [11].

Rheology is naturally another strong candidate to probe indirectly nanocomposites morphology. In fact, several studies (see recent review [17]) reported a direct correlation between the degree of dispersion and the level of interfacial interactions between the silicate and the matrix with the linear rheological properties. The storage modulus, $G'(\omega)$ was found to increase with increasing degree of dispersion over the entire frequency range [18]. In fact, a gradual change of behavior from liquid-like to solid-like, with the presence of a low frequency plateau on storage modulus, has been observed and mainly attributed to the extent of dispersion [18], although an exact association with intercalation and/or exfoliation states is still missing. Similarly, under extensional uniaxial elongational flow, a tendency to stronger strainhardening for higher dispersion levels seems to exist [17].

Scanning Electron Microscopy, SEM and, especially, Transmission Electron Microscopy, TEM, provide a unique opportunity to directly visualize nanocomposite morphology. Despite of requiring good skills and being labor intensive, if various images are captured and this is done at various magnifications, these techniques can provide a representative perception of the morphology being analysed. Therefore, the present study aims to take advantage

of these techniques to better understand the dispersion mechanisms of layered clays in polymer blend matrices, as well as to investigate the compatibilization effect of these fillers. A Polyamide 6 / Polypropylene, PA6/PP, blend was selected as a model system, both in its immiscible and compatibilized forms (i.e., with the addition of PP grafted with maleic anhydride). The two blends were compounded with two commercial montmorillonite organoclays, the morphology evolution being characterized along the extruder axis.

Materials and experimental procedure

A Polyamide 6, PA6 (DOMAMID 27 from Atofina, with MFI value ranging between 17 and 23 $g/10\ min$, at $235^{\circ}C$ and 2.16 kg), and a Polypropylene homopolymer, PP (MOPLEN - HP502N from Basell, with MFI value of $12\ g/10\ min$ at $230^{\circ}C$ and 2.16 kg) were used as components of the immiscible blend. PP grafted with maleic anhydride, MA, containing $1\,wt.\%MA$, was supplied by Arkema (Orevac CA 100, with a MFI of $150\ g/10\ min$ at $230^{\circ}C$ and 2.16 kg). The organoclays selected (Cloisite 15A and 30 B , manufactured by Southern Clay Products, Inc.), consist of a montmorillonite modified organically with quaternary alkylammonium salts. Table 1 shows the composition of the blends and nanocomposites prepared for this research. Before compounding, PA6 and the nanoclays were dried under vacuum at $80^{\circ}C$ during 12-16 hours, and then tumble-mixed with PP or PP-g-MA.

Both the blends and the nanocomposites were prepared by melt compounding in a Leistritz LSM 30.34 intermeshing co-rotating twin screw extruder (screw diameter, $D=30\ mm$) under fixed operating conditions (barrel and die set uniformly at $230^{\circ}C$, screws rotating at 200 rpm and an output of $4\ kg/h$ set by a K-Tron gravimetric feeder). The screws are 29D long and contain four mixing zones separated by conventional conveying elements. Accordingly, as the material progresses towards the die, it must flow along 12 kneading disks followed by a left-handed element, four kneading disks, three kneading disks and a left handed element, respectively. All the kneading blocks are staggered negatively (-30°). Such a highly restrictive screw profile should be adequate to ensure the necessary dispersion levels, while avoiding polymer degradation. As for the extruder barrel, it was fitted with a number of sample collecting devices, which enable the removal of material from inside the extruder upon operation in approximately 1 second. They are located close to screw regions where positive pressure develops, not only for the reason that sample collection is quicker, but also because one would anticipate that chemical and/or morphological evolutions should develop here more significantly. The samples collected were immediately quenched in liquid nitrogen.

Table 1 Blends composition

Blends	PA6 (wL. %)	PP (wL. %)	PP-g-MA (plr)	Clay (phr)	
				C15A	C30B

PA6/PP	70	30	0	0	0
PA6/PP/PP-g-MA	70	30	5	0	0
PAG'PP/Clay	70	30	0	5	0
PA6/PP/Clay	70	30	0	0	5
PA6/PP/PP-g-MA/Clay	70	30	5	5	0
PA6/PP/PP-g-MA/Clay	70	30	5	0	5

The morphology of the blends and nanocomposites was analyzed using a Leica Cambridge S 360 Scanning Electron Microscope. Beforehand, the samples were fractured in liquid nitrogen, etched with hot xylene to remove the PP and covered with a thin gold layer. At least 200 particles of the dispersed phase were taken into consideration when estimating their average particle with the Image Pro-plus 4.5 software. Samples were also analyzed by means of a JEOL-JEM 1010 Transmission Electron Microscope (operating with a voltage of 100 kV). In this case, slices of the samples with thicknesses smaller than 90 nm were obtained by cryo-ultramicrotomy (at $-45^{\circ}C$, under liquid nitrogen), using a diamond knife, which were subsequently stained with ruthenium tetraoxide (RuO_4) vapour during 6 hours at room temperature.

Results and discussion

Figure 1 presents the morphology of the various blends prepared by melt mixing, as observed by SEM after PP extraction. In all cases, an homogeneous morphology consisting of nearly spherical PP droplets suspended in a PA6 matrix can be observed. However, and even though good dispersion levels have also been reached, the size of the dispersed phase is smaller when modified PP, nanoclay, or both, were added to the PA6/PP blend. The dimensional characterization of the dispersed PP particles is made in Table 2, in terms of the average equivalent particle size and standard deviation. The latter can be seen as an indication of the breath of the particle size distribution. The addition of 5 phr of PP-g-MA to PA6/PP decreases the average particle size of the dispersed phase from $10\,\mu\ m$ to $1.5\,\mu\ m$. The decrease is higher when only nanoclay (either Cloisite C15A or C30B) is added, as the average particle size reduces to circa 570 nm (573 nm for Cloisite C15A, 567 nm for C30B). Interestingly, the average particle size becomes even smaller when modified PP (PP-g-MA) and nanoclay are added together (338 nm and 411 nm for Cloisite C15A and C30B, respectively).

The decrease of the size of the dispersed phase due to the addition of PP-g-MA has been extensively reported in the literature and is generally attributed to the formation of a block copolymer at the interface, involving the amine groups of the PA6 and the anhydride groups of the PP-g-MA [19]. This block copolymer acts as

a compatibilizer, as it reduces the interfacial tension and stabilizes the morphology formed, preventing coalescence.

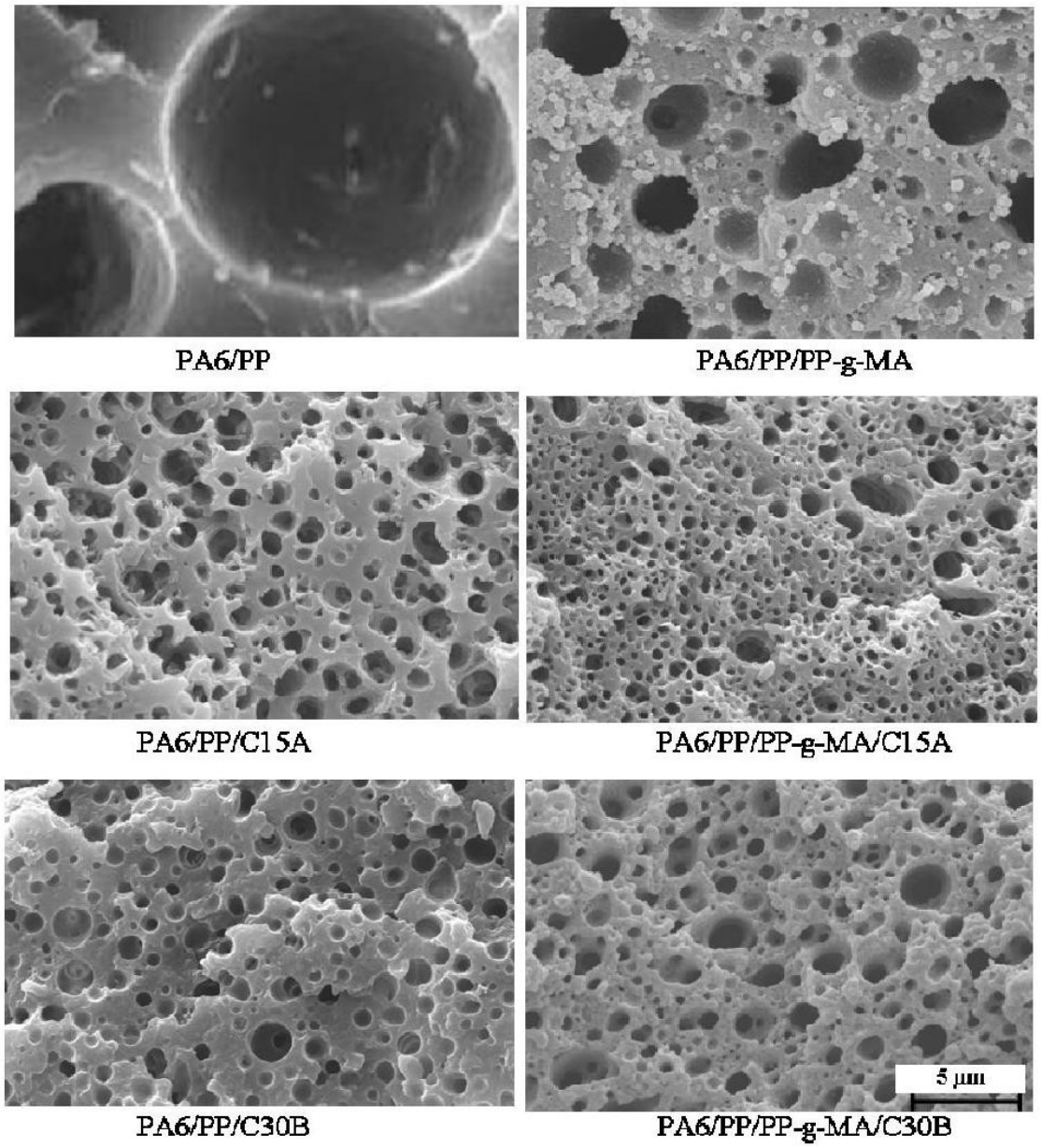

Fig. 1 SEM micrographs of the various blends

Table 2 Average diameter of the PP dispersed phase

PA6/ PP	PA6/PP/ PP-g-MA	PA6/PP/ C15A	PA6/PP/ PP-g-MA/C15A	PA6/PP/ C30B	PA6/PP/ PP-g-MA/C30B

10034 ± 4	1472 ± 348	573 ± 346	338 ± 214	567 ± 350	410 ± 331

In order to gain a better insight into the possible compatibilization effect of Cloisite C15A and C30B, TEM was used to identify the location of the silicate layers in the polymer blend morphology. Figures 2 and 3 refer to PA6/PP/C15A and PA6/PP/PP-g-MA/C15A blends, respectively, showing morphology details at different magnifications. As the samples were stained with ruthenium tetraoxide, the silicate layers appear as dark grey lines and PA6 and PP are the dark and light grey phases, respectively. The micrographs of Figures 2a and 3a are in good agreement with those obtained by SEM and shown in Figure 1, i.e., the PP particles are suspended in the PA6 matrix. The silicate layers are clearly visible in the TEM images. While in the blend without modified PP the layers are mainly deposited in the polyamide phase (Figure 2), in the compatibilized blend they can be distinguished both in the polyamide phase and at the interface between the two polymers (Figure 3). In neither case, were nanoclays observed in the PP phase.

Cloisite C15A has higher affinity with polar polymers containing polar groups and, henceforth it is reasonable that it concentrates mostly in PA6 and PP-g-MA, as confirmed in previous reports [20-27]. The higher magnification images demonstrate that clay dispersion is poor, having mostly reached an intercalation stage, as it is possible to discern multiple layers packed together. This dispersion inefficiency is most probably associated with the low chemical affinity of Cloisite C15A to PA6, since this clay is modified with non-polar groups.

Even though similar images were obtained with Cloisite C30B (Figures 4 and 5), the dispersion situation is different. As with Cloisite C15A, the silicate layers are either selectively dispersed in the PA6 phase (Figure 4), or in PA6 and at the interface (Figure 5) when PP-g-MA is added. However, higher magnification images reveal that the nanoclays are mostly exfoliated, as individual layers are perceived at the nano scale. This behavior should be due to the presence of OH groups in the organic part of Cloisite 30 B , which increase its chemical affinity with PA6.

Taking into consideration the above observations, it seems that the differences in particle size of the blends containing silicate layers (see Figure 1) appear to be related to the amount of organoclay located at the interface between the two polymer blend constituents. The higher this amount, the smaller the particle size. When PP-g-MA is added to the PA6/PP blend, the quantity of nanoclay situated at the interface increases (Figures 3c and 4c), resulting in further reduction of the particle size. Similar observations have been previously reported and attributed to a joint compatibilization effect of PP-g-MA and organoclay [28-33]. In what concerns the organoclay, the compatibilization effect could be due to the physical interaction promoted by the presence of the high aspect ratio silicate nanolayers.

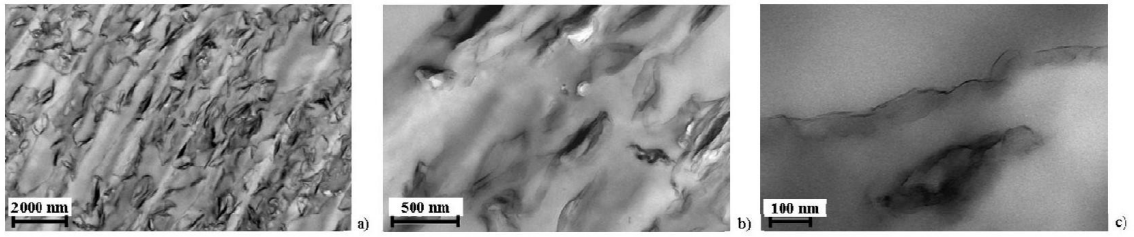

Fig. 2 TEM micrographs of PA6/PP/C15A blends at different magnifications

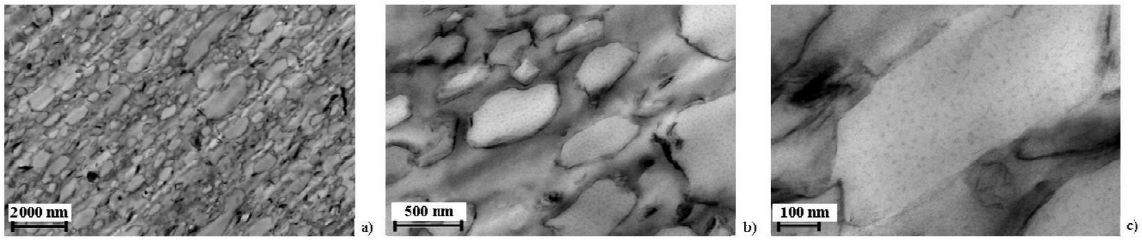

Fig. 3 TEM micrographs of PA6/PP/PP-g-MA/C15A blends at different magnifications

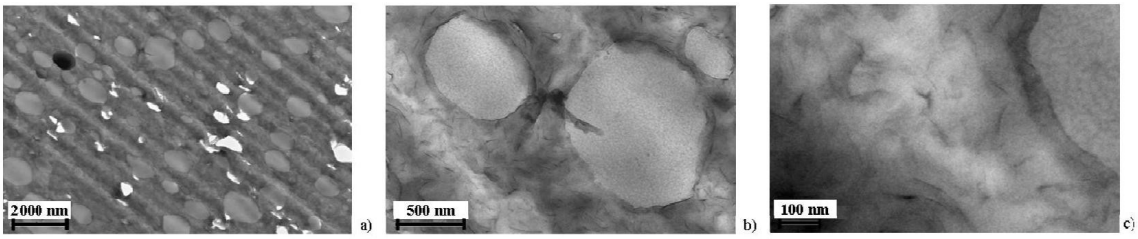

Fig. 4 TEM micrographs of PA6/PP/C30B blends at different magnifications

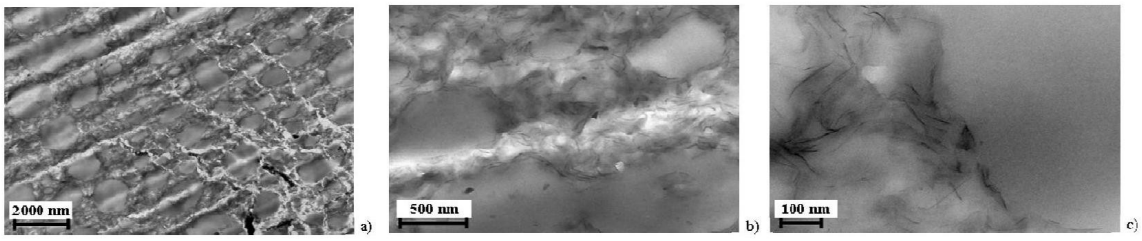

Fig. 5 TEM micrographs of PA6/PP/PP-g-MA/C30B blends at different magnifications

Figure 6 depicts the evolution of the morphology of the PA6/PP/PP-g-MA/C15A blend along the extruder (locations L/D=8.8 and 10 along the screw) and at the die exit. Phase inversion seems to take place between L/D=8.8 and L/D=10, due to melting of all PA6. At L/D = 10 the morphology seems to have reached a relative stability, as it is quite similar to that of the extrudate. In all micrographs, the clay seems to concentrate in the PA matrix and at the interface, which means

that the process begins quite early in the screw and is nor affected by the phase inversion.

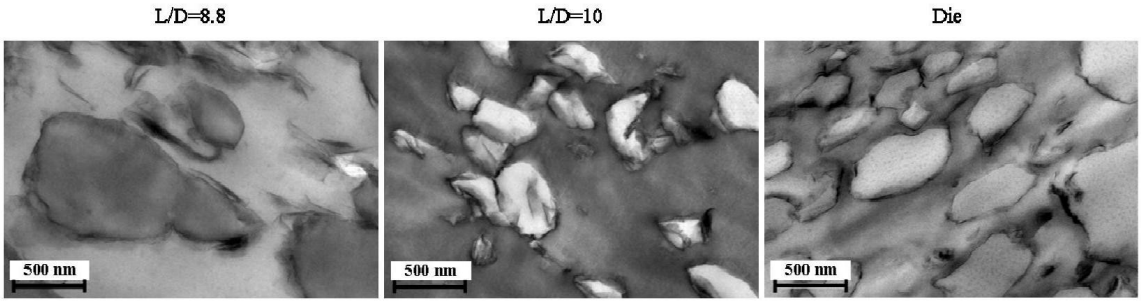

Fig. 6 TEM micrographs of PA6/PP/PP-g-MA/C15A along the extruder.

Conclusions

This study used SEM and TEM to investigate the dispersion mechanisms of layered clays in polymer blend matrices and to identify and explain the eventual compatibilization effect of these fillers. A Polyamide 6 / Polypropylene 70/30 w/w immiscible blend was compatibilized with modified PP and filled with one commercial montmorillonite organoclay (Cloisite C15A or Cloisite C30B) using twin-screw melt compounding. The dispersion of the layered silicate into the polymer matrix and its compatibilization effect were investigated along the screw axis and at the die exit.

The addition of PP-g-MA, of nanoclay and of the two together to PA6/PP decreased progressively the average particle size of the dispersed phase. The effect of the addition of PP-g-MA is due to the formation of a block copolymer at the interface. It was speculated that the organoclay promoted a physical interaction due to the presence of the high aspect ratio silicate nanolayers.

Acknowledgements The authors are grateful to Portuguese Foundation of Science and Technology (FCT) for financial support (SFRH/BD/31543/2006).

References

[1] Huang XY, Lewis, S Brittain WJ, Vaia, RA. Synthesis of polycarbonate-layered silicate nanocomposites via cyclic oligomer. Macromolecules. 2000;33:2000-2004.
[2] Su S, Jiang DD, Wilkie CA. Poly(methyl methacrylate), polypropylene and polyethylene nanocomposites formation by melt blending using novel polymerically-modified clay. Polymer Degradation and Stability. 2003;83:321-331.
[3] Tang Y, Hu Y, Zhang R, Gui Z, Wang ZZ, Chen ZY, Fan WC, Fan W. Investigation on polypropylene and polyamide-6 alloys/montmorillonite nanocomposites. Polymer. 2004;45:5317-5326.
[4] Ray SS, Bousmina M. Poly(butylene sucinate-co-adipate)/montmorillonite

nanocomposites: effect of organic modifier miscibility on structure, properties, and viscoelasticity. Polymer. 2005;46:12430-12439.
[5] Zhang J, Jiang DD, Wilkie CA. Thermal and flame properties of polyethylene and polypropylene nanocomposites based on an oligomerically-modified clay. Polymer Degradation and Stability. 2005;91:298-304.
[6] Vermogen A., Masenelli-Varlot K, Seguela R, Duchet-Rumeau J, Boucard S, Prele P. Evaluation of the structure and dispersion in polymer-layered silicate nanocomposites. Macromolecules. 2005;38:9661-9669.
[7] Ryu SH, Chang Y-W. Factors affecting the dispersion of montmorillonite in LLDPE nanocomposite. Polymer Bulletin. 2005;55:385-392.
[8] Cao X, Lee LJ, Widya T, Macosko C. Polyurethane/clay nanocomposites foams: processing, structure and properties. Polymer. 2005;46:775-783.
[9] Wang K, Chen Y, Zhang Y. Effects of organoclay platelets on morphology and mechanical properties in PTT/EPDM-gMA/organoclay ternary nanocomposites. Polymer. 2008;49:3301-3309.
[10] Durmus A., Kasgoz A, Macosko CW. Mechanical properties of linear low-density polyethylene (LLDPE)/clay nanocomposites: Estimation of aspect ratio and interfacial strength by composite models. Journal of Macromolecular Science Part B-Physics. 2008;47:608-619.
[11] Paul DR, Robeson LM. Polymer nanothechnology: nanocomposites. Polymer. 2008;49:3187-3204.
[12] Özkoç G, Bayram G, Quaedflieg M. Effects of microcompounding process parameters on the properties of ABS/polyamide-6 blends based nanocomposites. Journal of Applied Polymer Science. 2007;107:3058-3070.
[13] Dasari A, Yu ZZ, Mai YW. Effect of blending sequence on microstructure of ternary nanocomposites. Polymer. 2005;46:59865991.
[14] Li K, Huang H-X, Jiang G. Comparing the continuous chaotic and shear mixing-induced morphology development of polyblend and its nanocomposites. Polymer-Plastics Technology and Engineering. 2009;48:989-995.
[15] Gahleitner M, Kretzschmar B, Pospiech D, Ingolic E, Reichelt N, Bernreitner K. Morphology and mechanical properties of polypropylene/polyamide6 nanocomposites prepared by two-step melt-compounding process. Journal of Applied Polymer Science. 2006;100:283-291.
[16] Morgan AB, Gilman JW. Characterization of polymer-layered silicate (clay) nanocomposites by transmission electron microscopy and x-ray diffraction: A comparative study. Journal of Applied Polymer Science. 2003;87:1329-38.
[17] Ray SS. Rheology of polymer/layered silicate nanocomposites. Journal Ind Engineering and Chemistry. 2006;12:811-842.
[18] Ray SS, Okamoto K, Yamada K, Okamoto M. New polylactide/layered silicate nanocomposites. 1. Preparation, characterization, and properties. Macromolecules. 2002;35:3104-3110.
[19] Machado AV, Covas JA, Duin M. Chemical and morphological evolution of PA-6/EPM/EPM-g-MA blends in a twin screw extruder. Journal Polymer Science: Part A: Polymer Chemistry. 1999, 37, 1311-1320.
[20] Chow WS, Ishak ZAM, Karger-Kocsis J. Morphological and rheological properties of polyamide6/poly(propylene)/organoclay nanocomposites. Macromolecular. Materials and engineering. 2005;290:122-127.

[21] Su QS, Feng M, Zhang SM, Jiang JM, Yang MS. Melt blending of polypropylene-blend-polyamide 6-blend-organoclay systems. Polymer International. 2007;56:50-56.
[22] Chow WS, Ishak ZA.M, Karger-Kocsis J, Apostolov AA, Ishiaku US. Compatibilizing effect of maleated polypropylene on the mechanical properties and morphology of injection molded polyamide 6/polypropylene/organoclay nanocomposites. Polymer. 2003;44:7427-7430.
[23] Chow WS, Abu Bakar A, Ishak ZA.M, Karger-Kocsis J, Ishiaku US. Effect of maleic anhydride-grafted ethylene-propylene rubber on the mechanical, rheological and morphological properties of organoclay reinforced polyamide 6/polypropylene nanocomposites. European Polymer Journal. 2005;41:687-696.
[24] Othman N, Hassan A, Rahmat AR, Wahit MU. Preparation and characterisation of polyethylene-octene grafted maleic anhydride-toughened 70:30 PA6/PP/MMT nanocomposites. Polymers & Polymer Composites. 2007;15:217-227.
[25] Chow WS, Ishak ZA.M, Ishiaku US, Karger-Kocsis J, Apostolov AA. Compatibilizing effect of maleated polypropylene on the mechanical properties and morphology of injection molded polyamide 6/polypropylene/organoclay nanocomposites. Journal of Applied Polymer Science. 2003;91:175-189.
[26] Khatua BB, Lee DJ, Kim HY, Kim JK. Effect of organoclay platelets on morphology of nylon-6 and poly(ethylene-ranpropylene) rubber blends. Macromolecules. 2004;37:2454-2459.
[27] Yang JT, Sun L, Xiang SF, He JL, Gu LC, Zhong MQ. Influence of organoclay and preparation technique on the morphology of polyamide6/polystyrene/organoclay nanocomposites. Journal of Applied Polymer Science. 2008;110:276-282.
[28] Chen GX, Kim HS, Kim ES, Yoon JS. Compatibilization-like effect of reactive organoclay on the poly(L-lactide)/poly(butylene succinate) blends. Polymer. 2005;46:11829-11836.
[29] Fang Z, Harrats C, Moussaif N, Groeninckx G. Location of a nanoclay at the interface in an immiscible poly(epsiloncaprolactone)/poly(ethylene oxide) blend and its effect on the compatibility of the components. Journal of Applied Polymer Science. 2007;106:3125-3135.
[30] Elias L, Fenouillot F, Majeste JC, Cassagnau P. Morphology and rheology of immiscible polymer blends filled with silica nanoparticles. Polymer. 2007;48:6029-6040.
[31] Ray SS, Pouliot S, Bousmina M, Utracki LA. Role of organically modified layered silicate as an active interfacial modifier in immiscible polystyrene/polypropylene blends. Polymer. 2004;45:8403-8413.
[32] Ray SS, Bandyopadhyay J, Bousmina M. Effect of organoclay on the morphology and properties of Poly(propylene)/Poly[(butylene succinate)-co-adipate] blends. Macromolecular Materials and Engineering. 2007;292:729-747.
[33] Hong JS, Namkung H, Ahn KH, Lee SJ, Kim C. The role of organically modified layered silicate in the breakup and coalescence of droplets in PBT/PE blends. Polymer. 2006;47:3967-3975.